Fast Excitatory Nicotinic Transmission in the Chick Lateral Spiriform Nucleus

Yi Nong, Eva M. Sorenson, and Vincent A. Chiappinelli

Department of Pharmacology, The George Washington University Medical Center, Washington, DC 20037

The lateral spiriform nucleus (SpL) in the chick mesencephalon contains functional nicotinic receptors and receives a cholinergic fiber projection. We now use double-label immunohistochemistry to demonstrate that choline acetyltransferase-immunopositive fibers in the SpL and in the cholinergic fiber tract lateral to the nucleus are associated with fibers expressing the α5 and/or α3 nicotinic receptor subunits as determined by mAb35 immunoreactivity. This morphological evidence suggests that there might be synapses between the cholinergic fibers and the dendrites of SpL neurons. Whole-cell recordings from SpL neurons in current-clamp mode revealed EPSPs evoked by stimulation of the cholinergic fiber tract lateral to the SpL. These EPSPs increased in amplitude in the presence of bicuculline. Further addition of the nicotinic antagonist dihydro-β-erythroidine (DHβE) to the buffer significantly attenuated them. Almost all of the remaining EPSP was blocked by 6,7-dinitroquinoxaline-2,3-dione. In the presence of an antagonist cocktail that isolated the nicotinic responses, a fast, monosynaptic nicotinic EPSP or EPSC was evoked. In some neurons, the nicotinic EPSP resulted in the generation of an action potential. The nicotinic nature of the evoked response was confirmed by blockade of the EPSPs or EPSCs with nicotinic antagonists, including DHβE, D-tubocurare, and mecamylamine. The nicotinic response was insensitive to low concentrations (10–100 nM) of methyllycaconitine, indicating that typical α7-containing receptors were not involved. The results demonstrate that endogenously released acetylcholine generates EPSPs that can elicit action potentials by acting at postsynaptic nicotinic receptors on SpL neurons.

Key words: nicotinic; evoked; neurotransmission; lateral spiriform nucleus; cholinergic; α5 nicotinic receptor subunit

Several types of central neurons are known to express postsynaptic nicotinic receptors as evidenced by recording of nicotinic potentials or currents in response to exogenous nicotinic agonists and blockade of these responses by nicotinic antagonists. However, there are few reports of fast synaptic nicotinic neurotransmission in brain (Role and Berg, 1996). We have previously chosen the chick lateral spiriform nucleus (SpL) as a likely nucleus to contain nicotinic cholinergic synapses based on the findings that the SpL receives a cholinergic projection and that SpL neuronal cell bodies and processes have among the highest densities of ^{3}H-nicotine binding sites in the brain (Sorenson et al., 1989; Sorenson and Chiappinelli, 1992). Intracellular recordings with sharp electrodes demonstrated that activation of nicotinic receptors with exogenous agonists caused SpL neurons to depolarize and generate action potentials (Sorenson and Chiappinelli, 1990). Further studies using whole-cell patch-clamp recordings have found that the nicotinic receptors on SpL neurons are likely to consist of more than one combination of nicotinic receptor subunits because they have differential sensitivities to trimethaphan and show four different sizes of single-channel currents (Weaver et al., 1994; Weaver and Chiappinelli, 1996). Nicotinic agonists were found to have presynaptic, as well as postsynaptic, effects because they increased the frequency of spontaneous GABAergic IPSCs recorded from SpL neurons (McMahon et al., 1994).

A study by Ullian and Sargent (1995) returned the focus of our attention to the cholinergic afferents to the SpL. These authors suggested that most of the nicotinic receptors on SpL neurons are not localized at synapses on the somata of SpL neurons as shown by double-label immunofluorescence for individual nicotinic receptor subunits and a synaptic vesicle protein. We wanted to take their study one step further and determine whether the cholinergic afferents in the SpL were associated with structures containing nicotinic receptors. We have begun by examining the double labeling of the SpL with mAb35 for the α3/α5 nicotinic receptor subunits and antiserum against choline acetyltransferase (ChAT) (the synthetic enzyme for acetylcholine). We now report that ChAT-positive afferents are associated with mAb35-immunopositive fibers, some of which appear to be processes of SpL neurons. To further test the hypothesis that cholinergic afferents synapse onto the dendrites of SpL neurons, we have stimulated the cholinergic fiber tract lateral to the SpL while performing whole-cell patch-clamp recording from SpL neurons. The electrophysiological results establish that SpL neurons receive fast synaptic neurotransmission mediated by nicotinic receptors.

MATERIALS AND METHODS

Immunohistochemistry. Three newly hatched White Leghorn chicks (Truslow Farms, Chestertown, MD) were decapitated, and their brains were removed. The mesencephalon was dissected out and submersion-fixed in 1% paraformaldehyde in 0.1 M phosphate buffer for 4 hr at 4°C. The brains were then put in either 30% sucrose for cryoprotection or 0.1 M PBS, pH 7.35, until sectioning. Transverse sections containing the SpL were cut on a cryostat (50 μm) or on a vibratome (100 μm). The sections were double or single immunolabeled for ChAT and/or the α5/α3 nico-

Received April 19, 1999; revised June 18, 1999; accepted June 28, 1999.

This research was supported by National Institutes of Health Grant NS 17574 to V.A.C. We thank Miles L. Epstein for his generous contribution of anti-ChAT antiserum.

Drs. Nong and Sorenson contributed equally to this work.

Correspondence should be addressed to Dr. Vincent A. Chiappinelli, Department of Pharmacology, The George Washington University Medical Center, 2300 Eye Street NW, Washington, DC 20037.

tinic receptor subunits. Specifically, free-floating sections were washed and then incubated with one or both of the primary antibodies for 24–72 hr. The primary antiserum for choline acetyltransferase, a rabbit antiserum against the chicken enzyme, was the generous gift of Miles Epstein (University of Wisconsin) (Johnson and Epstein, 1986). It is well characterized and has been previously used in our laboratory (Sorenson et al., 1989). mAb35 is a rat monoclonal antibody that recognizes the α1, α3, and α5 nicotinic receptor subunits (Research Biochemicals, Natick, MA) (Tzartos et al., 1981). It also is well characterized and has been used for immunolabeling nicotinic receptors in the chick brain, particularly in the SpL (Swanson et al., 1983; Ullian and Sargent, 1995). The dilution for the ChAT antiserum was 1:2500 or 1:5000, and for mAb35 it was 1:6600. The incubation buffer consisted of 0.1 M PBS containing 5% normal goat serum and 0.3% Triton X-100. The sections were given three washes in PBS and then incubated overnight in buffer containing both secondary antibodies. The secondary antibodies were produced in goat. The anti-rabbit antibody was conjugated to Cy3 and the anti-rat antibody was conjugated to Cy5 (Jackson ImmunoResearch, West Grove, PA). After washing, the sections were mounted on slides and coverslipped using 90% glycerol, 10% PBS, and 4% propyl gallate as the mounting medium. Coverslips were sealed with fingernail polish and stored in the dark at 4°C until imaging. Specificity was determined by omitting either one or both of the primary antibodies from the incubations or by omitting the secondary antibodies.

Imaging was done on a Bio-Rad (Hercules, CA) MRC-1000 confocal microscope equipped with a krypton–argon laser. Cy3 was excited with the 568 nm excitation line of the laser, and emissions were collected using emission filter 605/32. Cy5 was excited with the 647 nm line of the laser, and emission was collected using the 680/32 filter. The laser was attenuated with a 3, 10, or, occasionally, 30% transmission neutral density filter. Images were collected with either a 20 or 60× planapo objective with numerical apertures of 0.7 and 1.4, respectively. Image collection was done with signal averaging. Images were collected sequentially for the two different fluorophores in double-labeled sections. Scan speed, low-signal, and iris settings depended on the particular specimen under observation.

Electrophysiology. SpL slices (400 μm) were prepared from chick embryos at 18 d of incubation. Brain slices were cut with a vibrating tissue slicer in cold, oxygenated buffer. The composition of the external recording buffer was (in mM): 126 NaCl, 2.5 KCl, 2.5 $CaCl_2$, 1.3 $MgCl_2$, 1.2 Na_2HPO_4, 25 $NaHCO_3$ and 10 glucose bubbled with 95% O_2–5% CO_2. The slice was continuously superfused at 4 ml/min at room temperature. Drugs were applied by bath perfusion.

The SpL neurons were visualized with an Axioskop microscope (Zeiss, Jena, Germany) for whole-cell patch-clamp recording. Patch pipettes were made by a two-stage microelectrode puller and had a resistance of 4–7 MΩ after filling with an internal solution containing (in mM): 140 K-gluconate, 10 HEPES, 5.0 EGTA, 5 Mg-ATP, and 2 $MgCl_2$. QX314 (5 mM) was added to the pipette solution to block Na^+ transients when only voltage-clamp experiments were planned. Conventional patch-clamp techniques were used with an Axopatch-200B amplifier (Axon Instruments, Foster City, CA) in either the voltage- or current-clamp configurations. In voltage clamp, holding potential was between −60 and −70 mV. The series resistance (R_s) was calculated by adjusting the cell capacitance and R_s potentiometers on the amplifier. The R_s was 9.4 ± 0.9 MΩ (n = 25). The R_s compensation was set at 75–90% (lag, 10 μsec). Cholinergic afferents were stimulated at 0.05 Hz at an intensity between 100 and 900 μA and a duration of 100–900 μsec with a concentric bipolar electrode placed at the lateral side of the SpL. The distance between the bipolar and recording electrodes ranged from 0.2 to 1 mm. The EPSC or EPSP was recorded with a video cassette recorder (Vetter, Rebersburg, PA). The data were sampled by pClamp 6 software (Axon Instruments) through a Digidata 1200 DMA interface.

Analysis of evoked synaptic events was performed by Clampfit 6.03 software (Axon Instruments) and SigmaPlot 4.0 (SPSS Inc., Chicago, IL). Seven consecutive traces of evoked responses were averaged. The peak current amplitude was calculated by averaging three adjacent points at the peak. The decay time constants were determined using a simplex algorithm by fitting EPSCs with the exponential function $I = A * \exp(-t/\tau) + C$, where A is the amplitude coefficient, and τ is the decay time constant. In some cases, the sum of two exponential functions was used. Statistics were performed with SigmaStat version 1.0 (SPSS Inc). The data were expressed as mean ± SEM. Differences between means were examined by paired t test.

Drugs were obtained as follows: eserine, atropine sulfate, (−)-nicotine bitartrate, 6,7-dinitroquinoxaline-2,3-dione (DNQX), and bicuculline methiodide from Sigma (St. Louis, MO); 2-amino-5-phosphovalerate (AP-5), methyllycaconitine (MLA), and mecamylamine from Research Biochemicals; and D-tubocurare from Calbiochem (San Diego, CA). Dihydro-β-erythroidine (DHβE) was a gift from Merck, Sharp & Dohme Research laboratories (Rahway, NJ).

RESULTS

Colocalization of ChAT and mAb35

Single- or double-labeled sections treated with mAb35 contained mAb35-positive fibers in the tract lateral to the SpL (Fig. 1*A*,*C*). The cells in the SpL itself were heavily labeled with mAb35, but there were no labeled cells present within the cholinergic fiber tract lateral to the SpL. It was not possible to determine whether the mAb35-positive fibers lateral to the SpL originated from SpL neurons. Sections of the SpL single- or double-labeled for ChAT showed a cholinergic fiber tract lateral to the SpL as reported previously (Fig. 1*B*,*C*). Within the nucleus, a lower density of neuropil labeling was present, and no cells were immunopositive. Double-labeled sections had a high density of overlap of mAb35-positive fibers and ChAT-positive fibers in the tract lateral to the SpL (Fig. 1*C*). Portions of the nucleus farthest from the fiber tract appeared to have lower levels of ChAT fibers than the rest of the nucleus. At higher magnification, it was apparent that there was more interaction of ChAT-immunopositive fibers with mAb35-positive fibers in the tract lateral to the SpL than in the SpL itself (Fig. 1*D–F*).

Serial optical images through randomly selected neurons were obtained consecutively for mAb35 and ChAT immunolabeling. When the individual images were merged, it appeared that the ChAT labeling was predominantly associated with mAb35-positive fibers rather than the cell bodies (Fig. 2*A–F*). ChAT immunolabeling would follow, or dot, mAb35-labeled fibers, but there was little ChAT labeling at the surface of the cells. The ChAT- and mAb35-labeled fibers were not identical (Fig. 2*A–F*). Furthermore, neurons in the nucleus semilunaris, the source of the cholinergic afferents in the SpL, were immunopositive for ChAT but not for mAb35 (data not shown). Some of the mAb35-immunopositive fibers that originate from SpL neurons may be associated with ChAT fibers (Fig. 2*C*,*D*, *arrows*). Control sections in which the primary antibodies or secondary antibodies were omitted did not show any fluorescence.

Nicotinic receptors directly mediate fast excitatory neurotransmission

Whole-cell recordings were performed in visually identified SpL neurons (n = 127). Evoked monosynaptic responses were elicited by electrical stimulation (0.05 Hz) lateral to the SpL nucleus. EPSPs were elicited in 90% (36 of 40) of SpL neurons whose resting membrane potentials were held at −60 mV in the current-clamp mode. In some neurons, evoked EPSPs increased in amplitude with increasing stimulation intensities. In six of these SpL neurons, the EPSP reached threshold, and an action potential was generated (Fig. 3*A*, *left*). The action potential threshold was −49.2 ± 0.6 mV (n = 6). The mean height of the evoked action potentials was 59.7 ± 2.9 mV, and the width at half the maximum of the action potential was 1.76 ± 0.08 msec. The height of the action potential was determined by measuring from threshold to peak. DHβE (10–60 μM), a nicotinic antagonist, blocked the evoked spike but an EPSP remained (n = 3) (Fig. 3*A*, *right*). In the presence of an antagonist cocktail to isolate the nicotinic response, the nicotinic EPSP was large enough to generate an action potential in some neurons (n = 3) (Fig. 3*B*, *left*). The action

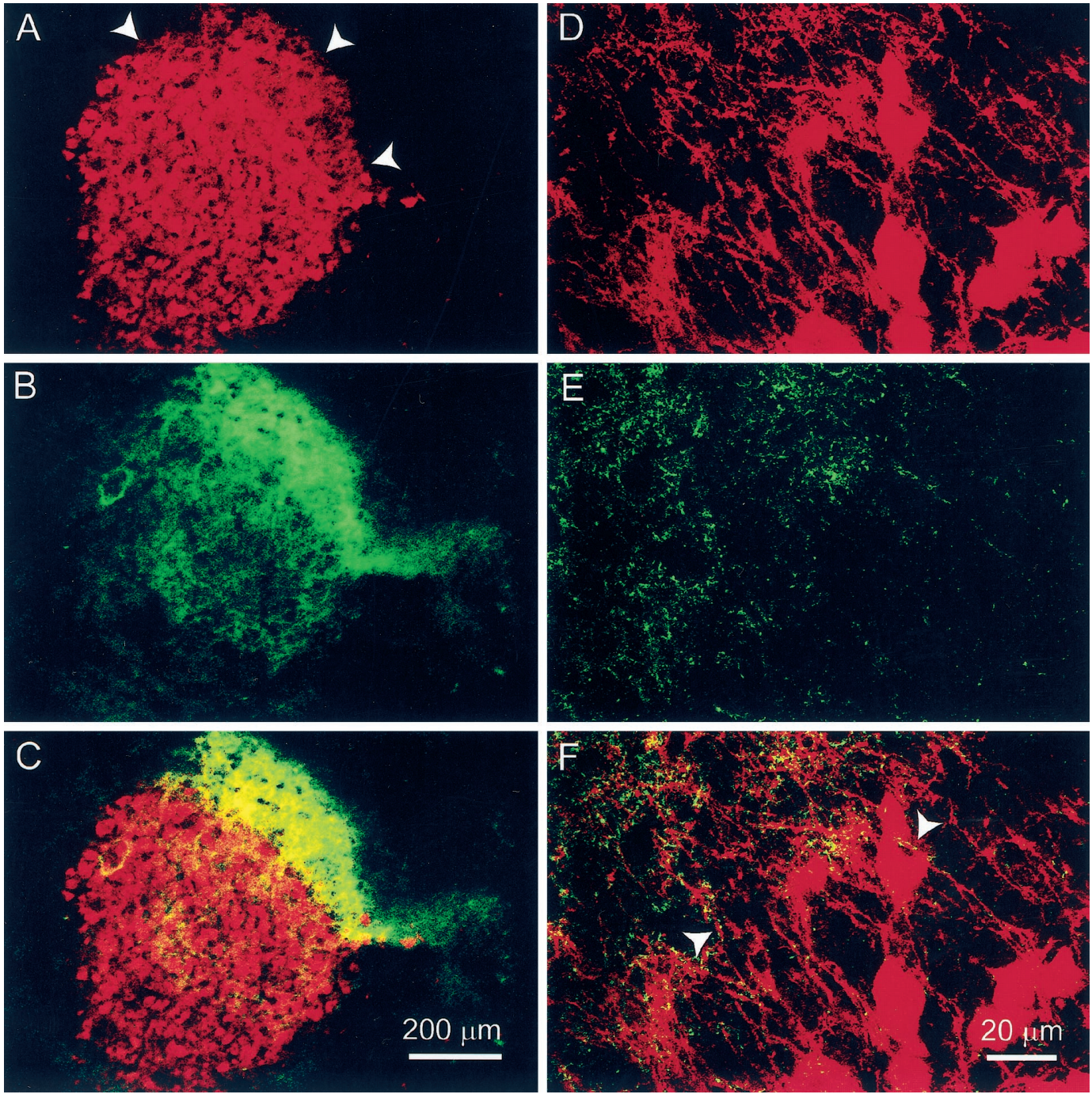

Figure 1. Localization of ChAT and the α3/α5 subunits in the SpL. Sections containing the SpL were double labeled with mAb35 and anti-ChAT antiserum. Sequential images of the labeling for each of the antigens were collected and merged to demonstrate areas of colocalization. mAb35 labeling is represented by *red*, ChAT by *green*, and colocalization by *yellow* in all images. *A–C*, At low magnification, mAb35 is seen to label most SpL neurons and also fibers lateral to the nucleus (*A*, *arrowheads*). A cholinergic fiber tract is immediately lateral to the nucleus, and cholinergic fibers emanate from the tract into the SpL (*B*). *C*, A merge of images *A* and *B*, demonstrates that mAb35-positive fibers are localized in the cholinergic fiber tract. The highest density of colocalization of the two antigens appears to be in the cholinergic fiber tract. *A–C* were collected at normal speed with the iris set at 4.9 mm. *D–F*, mAb35, anti-ChAT, and a merge of the mAb35 and anti-ChAT immunolabeling, respectively, in the same section. In the region in which the fiber tract meets the SpL, there appear to be more cholinergic fibers associated with mAb35-positive fibers within the fiber tract than with SpL neurons. The *arrowheads* in *F* point out mAb35-positive fibers dotted with ChAT immunoreactivity.

potential and underlying EPSP could, under these conditions, be blocked by addition of DHβE (30 μM) to the superfusion buffer ($n = 3$) (Fig. 3*B*, *right*). These results indicate that activation of nicotinic receptors by synaptically released acetylcholine produces excitatory postsynaptic potentials that can reach threshold and result in the generation of an action potential in SpL neurons.

In the presence of bicuculline (10 μM), a $GABA_A$ antagonist, 43% of neurons tested (17 of 40) generated action potentials after stimulation of afferents (Fig. 4*A*, *second trace*). DNQX (20–40 μM) blocked the evoked action potentials, but an EPSP was still present (Fig. 4*A*, *third trace*). Nearly all of the remaining EPSP was sensitive to DHβE (60 μM) (Fig. 4*A*, *last trace*). In the

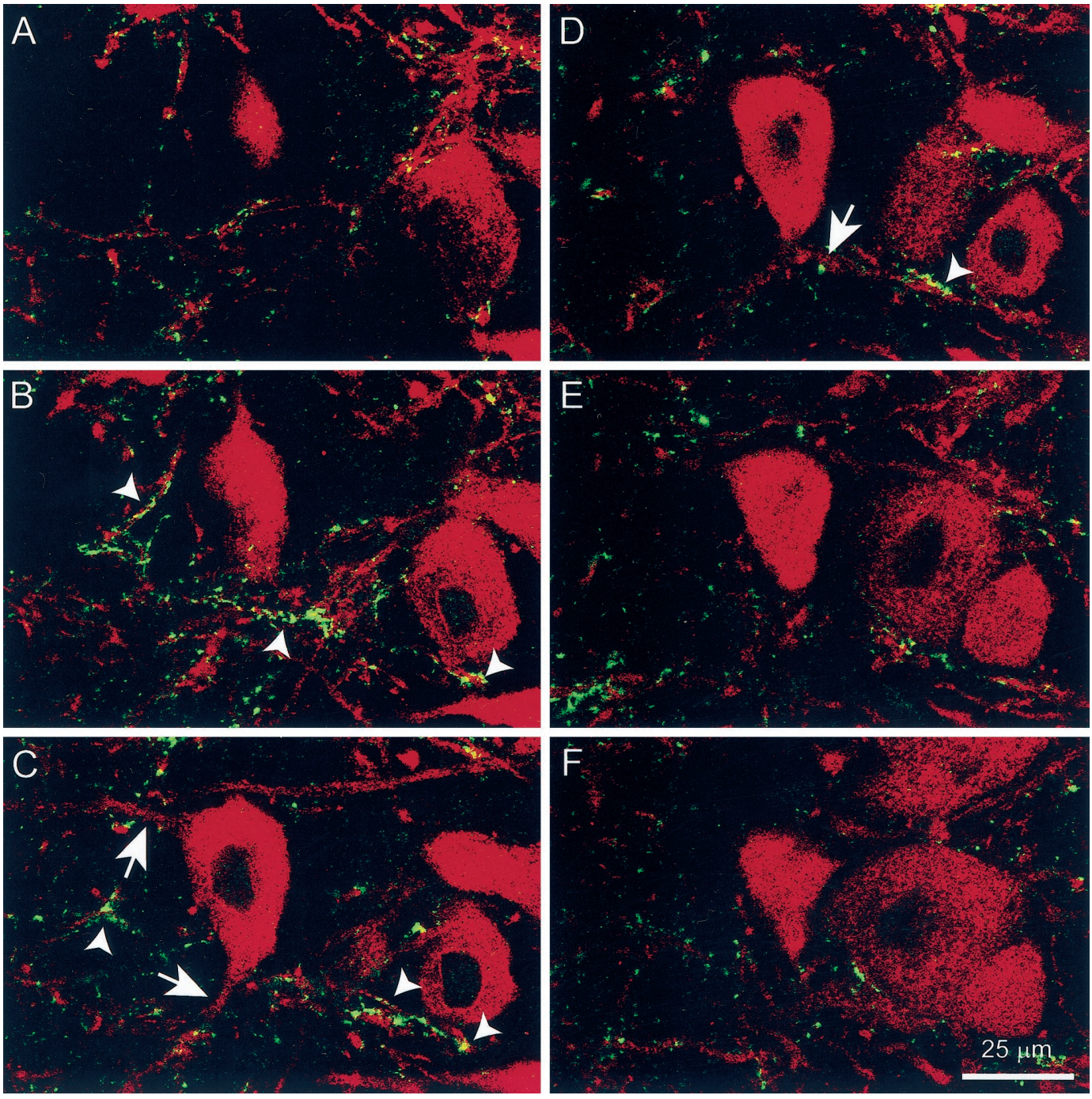

Figure 2. Cholinergic afferents in the SpL are associated with mAb35-immunopositive fibers. The figures are merged images of mAb35 and ChAT labeling at 1 μm intervals through a neuron in the SpL. Note that there do not appear to be ChAT-positive fibers associated with the surface of the SpL neuron. Rather, the ChAT labeling follows, or dots, the mAb35-positive fibers. *Arrowheads* show examples of areas in which the two antigens are in close proximity and may represent cholinergic synapses. *Arrows* indicate processes of the neuron that may be associated with ChAT fibers (*C*, *D*).

voltage-clamp mode, both outward and inward currents were recorded when the holding potential of the neurons was between −55 and −60 mV (Fig. 4*B*, *first trace*). Bicuculline (10 μM) blocked the outward current, indicating that it is mediated by $GABA_A$ receptors (Fig. 4*B*, *second trace*). The blockade of the outward current caused an increase in the amplitude of the inward current. A portion of the inward current was sensitive to DNQX (40 μM) (Fig. 4*B*, *third trace*), indicating that it was caused by activation of AMPA receptors. Nearly all of the remaining inward EPSC could be blocked by DHβE (60 μM) (Fig. 4*B*, *last trace*).

Properties of the evoked nicotinic response

To isolate the nicotinic EPSCs, the slice was superfused with the following antagonist cocktail (in μM): 50 AP-5, 40 DNQX, 10 bicuculline, and 1 atropine. Furthermore, in cells examined only in the voltage-clamp mode, QX314 (5 mM) was frequently added to the internal pipette solution to block transient Na^+ currents.

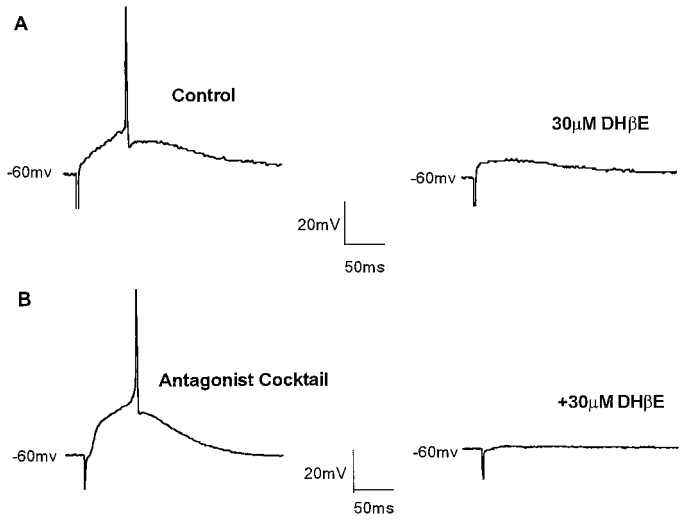

Figure 3. Excitatory synaptic transmission mediated by nicotinic receptors. *A*, An action potential was generated by electrical stimulation lateral to the SpL (*left*). Stimulation was at 0.05 Hz (450 μA, 300 μsec). The nicotinic receptor antagonist DHβE (30 μM) blocked the action potential but did not completely block the EPSP (*right*). *B*, In another SpL neuron, an antagonist cocktail containing AP-5 (50 μM), DNQX (40 μM), bicuculline (10 μM), and atropine (1 μM) was given to isolate the nicotinic response. The isolated nicotinic EPSP increased in amplitude with increasing stimulation intensity and, at 700 μA, 500 μsec (*left*), was sufficient to generate an action potential. DHβE (30 μM) completely blocked the action potential and EPSP (*right*).

Under these conditions, the sensitivity of the remaining EPSCs to a variety of nicotinic receptor antagonists was tested to help characterize the nicotinic receptor subtype(s) mediating synaptic transmission. DHβE (30 μM) significantly (83 ± 5.4%) reduced the EPSC amplitude ($n = 6$) (Fig. 5*A*). The blockade of nicotinic EPSCs by DHβE usually took 4–8 min, and complete recovery could be achieved by washing out DHβE for 20–30 min. D-Tubocurare (30 μM) blocked 85 ± 3.4% of the response amplitude in 3–5 min ($n = 6$) (Fig. 5*B*). The response recovered 40–60 min after washing out the D-tubocurare. Mecamylamine (10–20 μM) blocked 62–79% of the EPSC or EPSP amplitude in 10–15 min (Fig. 5*C*, $n = 4$). Mecamylamine was difficult to wash out, and 60–80 min were required for the response to recover completely after washout of drug was begun.

MLA is a selective antagonist of nicotinic receptors containing the α7 subunit in a concentration range of 10–100 nM (Alkondon and Albuquerque, 1993). At higher concentrations, MLA blocks all neuronal nicotinic receptors (Yum et al., 1996). In SpL neurons, MLA at 10–100 nM did not significantly decrease ($p > 0.05$; paired *t* test) the nicotinic EPSC amplitude ($n = 5$) (Fig. 5*D*, *left*). In contrast to low concentrations of MLA, 30 μM MLA did inhibit the nicotinic EPSCs by 54 ± 3.4% ($n = 4$) (Fig. 5*D*, *right*). These results suggest that the nicotinic receptors mediating synaptic transmission in SpL neurons do not contain α7 subunits.

The evoked nicotinic synaptic currents were detected after a delay of 1.0–3.2 msec after the stimulus artifact. The peak current amplitudes ranged between 10 and 117 pA with little variation between responses of the same neuron. The evoked nicotinic synaptic currents had a mean rise time of 6.7 ± 0.4 msec ($n = 20$) measured as the time required for the current to rise from 10 to 90% of the peak value. The decay phase of the currents could be fit well by a monoexponential function ($r^2 > 0.95$). The decay time constant ranged from 15.6 to 62.4 msec. The current–voltage relationship of the nicotinic EPSC is shown in Figure 5*E*. The current did not reverse itself but came to a plateau at ~0 mV. The extrapolated reversal potential is 0.6 mV ($n = 6$).

The effects of eserine on evoked EPSCs in the SpL

Eserine is an inhibitor of acetylcholinesterase, the degradative enzyme for acetylcholine. In the presence of 10 μM eserine, the amplitude of the EPSCs was reduced and the decay phase dramatically prolonged ($n = 6$). In the example shown in Figure 6*A*, the maximum amplitude was reduced from 117 to 72 pA, and the decay time constant (τ) was increased from 32.2 to 2898 msec. It took 60–80 min of washout to recover from the effects of eserine. At a lower concentration of 3 μM, eserine had less of an effect on the maximum amplitude but altered the decay rate to a two-exponential process ($n = 4$). In the example shown in Figure 6*B*, the maximum amplitude was 32.1 pA in control versus 28.7 pA in eserine. The single exponential rate of decay in control (τ value of 56.0 msec) changed to a two-exponential process in eserine with τ_1 of 38.9 msec and Amp_1 of 13.4 pA (56.8%), and τ_2 of 909 msec and Amp_2 of 10.2 pA (43.2%). After washing eserine out for 60 min, the decay rate was again a single exponential, similar to control (τ value of 62.1 msec).

DISCUSSION

The present study establishes that direct excitatory nicotinic transmission occurs in the mesencephalic SpL and characterizes the anatomical and functional elements of this central nicotinic synapse. Presynaptic cholinergic fibers arise from the nucleus semilunaris and form a fiber tract lateral to the SpL (present study; Sorenson et al., 1989). The cholinergic fiber density is highest in the fiber tract with individual ChAT fibers leaving the tract and entering the nucleus. Tract tracing studies using anterograde transport of tritiated amino acids have demonstrated that the fiber tract lateral to the SpL originates in the nucleus semilunaris (Reiner et al., 1982). However, based on the silver grain pattern they observed, Reiner et al. (1982) suggested that nucleus semilunaris innervated the area immediately lateral to the SpL and had only a slight projection to the SpL. The merged images of double-labeled sections in the present study also suggest that the cholinergic innervation of the SpL is not uniform. The areas of the SpL nearest the cholinergic tract appear to have more cholinergic fibers than the areas of the SpL farthest away from the tract.

The mAb35 immunolabeling suggests that the ChAT fibers may be interacting with mAb35-immunopositive fibers in the fiber tract lateral to the SpL. Our mAb 35 immunohistochemistry results confirm findings of mAb35 immunolabeling in the SpL previously reported in chicken (Swanson et al., 1983; Ullian and Sargent, 1995). However, mAb35 also recognized fibers in the cholinergic tract lateral to the SpL. The origin of the mAb35-positive fibers is not clear, nor is it known whether they are attributable to the presence of α5 versus α3 nicotinic receptor subunits. They could be processes from SpL neurons and/or afferents to the area that are also recognized by mAb35. We do not believe that the mAb35 fibers are identical to the ChAT fibers because there does not appear to be a one-to-one correspondence between them. In addition, in sections containing the nucleus semilunaris that were double-labeled with the mAb35 and ChAT antibodies, only ChAT labeling was present in the nucleus semilunaris. Watson et al. (1988) have also reported that ^{125}I-mAb35 did not bind to the nucleus semilunaris in the finch. Merged images of the double-labeled sections suggested that the greatest

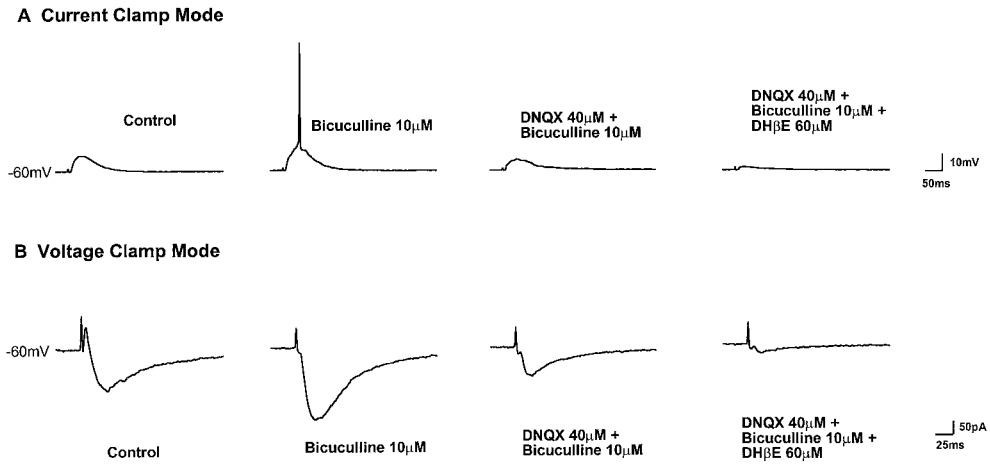

Figure 4. Evoked responses are mediated by nicotinic, glutamatergic, and GABAergic receptors. *A*, In current-clamp mode, electrical stimulation (450 μA, 300 μsec) lateral to the SpL elicits an EPSP in an SpL neuron (*first trace*). When $GABA_A$ receptors are blocked with bicuculline, the identical stimulus produces an action potential (*second trace*). Further addition of DNQX blocks the action potential (*third trace*), and most of the remaining EPSP is blocked by subsequent DHβE application (*last trace*). *B*, After a 55 min washout of all the antagonists, the experiment was repeated in voltage-clamp mode.

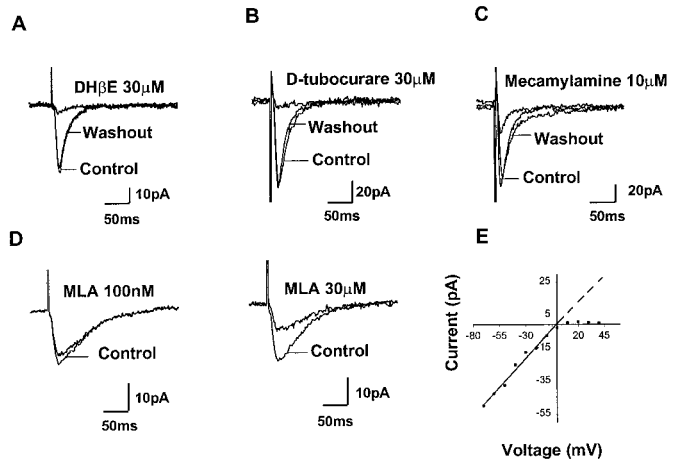

Figure 5. Properties of evoked nicotinic synaptic currents recorded from SpL neurons. The evoked responses shown in *A–E* were examined in the presence of an antagonist cocktail containing AP-5 (50 μM), DNQX (40 μM), bicuculline (10 μM), and atropine (1 μM) to isolate the nicotinic EPSCs. In *A–C*, superimposed traces of the evoked synaptic currents are shown for SpL neurons before (*Control*), during (*Drug*), and after (*Washout*) exposure to the indicated nicotinic antagonists. Holding potentials were −70 mV, and traces are averages of seven consecutive responses. In *D*, MLA (100 nM) did not inhibit the evoked nicotinic EPSCs (*left*). In contrast, 30 μM MLA significantly inhibited the evoked nicotinic EPSCs in the same neuron (*right*). In *E*, an *I–V* plot of the evoked nicotinic EPSCs was obtained in a SpL neuron. The nicotinic currents reversed near 0 mV and showed strong rectification at positive membrane potentials.

overlap of ChAT fibers with the mAb 35 immunoreactivity was in the lateral neuropil (Fig. 1). Images obtained at higher magnification within the SpL demonstrated that the ChAT-immunolabeled fibers were associated with mAb35-labeled fibers rather than cell bodies. When serial optical sections at 1 μm intervals in the z plane were obtained through individual SpL neurons, it appeared that there was little interaction of ChAT fibers with the surface of the somas; rather, the ChAT was associated with mAb35-immunoreactive fibers. Some of the ChAT-immunopositive fibers were associated with mAb35-immunopositive fibers that appeared to be processes of SpL neurons (Fig. 2), but whether all of the mAb 35 positive fibers originated in the SpL could not be established.

If, as the immunohistochemical data suggests, the mAb35-positive processes of SpL neurons are associated with ChAT afferents, we would predict that direct nicotinic responses could be evoked after stimulation of the cholinergic fiber tract. Indeed, after electrical stimulation in the cholinergic tract, three classes of monosynaptic responses could be distinguished with the appropriate antagonists: GABAergic, glutamatergic, and nicotinic. These synaptic potentials correspond to the known afferent projections to the SpL (Reiner et al., 1982). When the inhibitory $GABA_A$ currents were blocked with bicuculline, many of the SpL neurons exhibited an action potential after afferent stimulation. The SpL neurons therefore appear to be under a strong GABAergic inhibition. The GABAergic innervation could be caused by afferents from the paleostriatum primitivum (avian homolog of the globus pallidus) or the substantia nigra. It is also possible that some GABAergic SpL neurons innervate each other (Veenman and Reiner, 1994). The excitatory potentials recorded from the SpL neurons were mediated by glutamatergic and nicotinic receptors as evidenced by the blockade of the potentials by DNQX, AP-5, and DHβE. The cholinergic afferents, as has already been discussed, originate in the nucleus semilunaris, and the glutamatergic afferents project from the anterior ansa lenticularis, the avian homolog of the subthalamus (Medina et al., 1997).

Stimulation of cholinergic afferents in the SpL produces a fast excitatory nicotinic postsynaptic potential that can generate an action potential. The isolated synaptic response is nicotinic because it is blocked by nicotinic antagonists. In addition, blocking acetylcholinesterase with eserine altered the amplitudes and decay rates of the evoked response. Eserine also has direct effects on nicotinic receptors at concentrations required to block the enzyme (Mizobe and Livett, 1982; Shaw et al., 1985), and therefore the effects of eserine on nicotinic neurotransmission can be complex. The current–voltage relationship of the evoked nicotinic response behaves as others have reported for nicotinic receptors in that the extrapolated reversal potential is at 0.6 mV and the curve shows strong rectification at positive holding potentials. All of these results lead us to conclude that responses we recorded from SpL neurons were caused by fast excitatory nicotinic neurotransmission.

To date only a few examples of evoked fast nicotinic neurotransmission in the CNS are known. One is at hippocampal interneurons (Frazier et al., 1998; Alkondon et al., 1998). The nicotinic neurotransmission at hippocampal interneurons appears to be mediated by α7-containing nicotinic receptors because the response is blocked by 50–75 nM MLA. In contrast, the response we recorded from SpL neurons is not blocked by 100 nM MLA

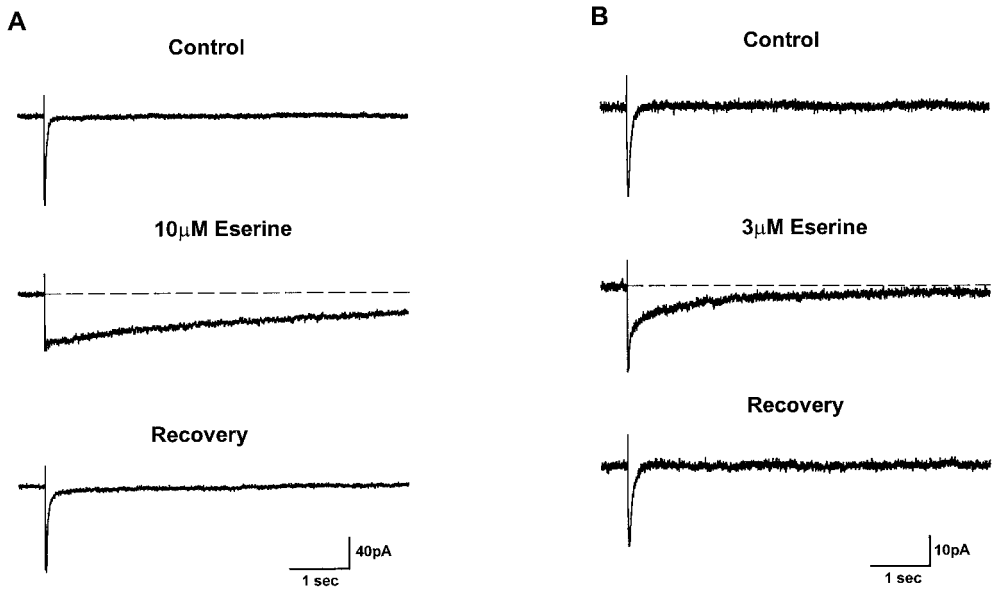

Figure 6. Effect of the acetylcholinesterase inhibitor eserine on evoked nicotinic EPSCs. Holding potential was −70 mV, and an antagonist cocktail containing AP-5 (50 μM), DNQX (40 μM), bicuculline (10 μM), and atropine (1 μM) was present throughout. All traces are averages of seven consecutive evoked responses. *A*, At 10 μM, eserine dramatically prolongs the decay phase of the EPSC and decreases the maximum current amplitude. *B*, At 3 μM, eserine has less of an effect on the maximum amplitude but alters the decay phase.

and requires concentrations of MLA (30 μM) that antagonize all classes of nicotinic receptors to observe inhibition. We have previously shown that somatic–dendritic nicotinic receptors on SpL neurons require 10–30 μM MLA for a blockade of activation by exogenous nicotinic agonists, whereas other central and ganglionic nicotinic receptors are blocked at significantly lower MLA concentrations (Yum et al., 1996). Although Ullian and Sargent (1995) found that up to 20% of SpL neurons expressed the α7 subunit, we did not observe evoked responses that were sensitive to low concentrations of MLA. Therefore, α7-containing receptors do not appear to be mediating the observed synaptic response and may be playing other functional roles in SpL neurons. For example, α7 receptors may also be localized on SpL terminals in the optic tectum in which they could modulate GABA release. Alternatively, it may be that we have not sampled enough neurons to detect the α7 receptor-mediated responses.

Another example of an evoked central nicotinic response is in the visual cortex of the ferret (Roerig et al., 1997). The nicotinic responses in the ferret were blocked by DHβE (50–100 μM) but not by α-bungarotoxin (100 nM), suggesting that they, like the responses presented here, are mediated by a non-α7-containing nicotinic receptor. Roerig et al. (1997) did not examine the evoked response in the current-clamp mode, so it is unclear whether the evoked nicotinic response could elicit action potentials.

The nicotinic receptors mediating the response in the SpL are likely to be made up of combinations of the α2, α5, and/or α4 subunits with the β2 subunits. All of these subunits are found in SpL, and the α2 and α5 subunits have the highest level of expression at 18–19 d of incubation in the chick embryo (Daubas et al., 1990; Ullian and Sargent, 1995). Most SpL neurons appeared immunoreactive for mAb35 in the present study as well. The results of three different experimental approaches have indicated that there are no α3 subunits in SpL neurons, so the mAb35 binding is to the α5 subunit. Ullian and Sargent (1995) concluded that the mAb35 was binding to the α5 nicotinic subunit because an antibody specific for the α3 subunit did not bind to SpL neurons. I*n situ* hybridization has not found mRNA for the α3 subunit in SpL neurons (Morris et al., 1990), and there is very little ^{125}I-κ-bungarotoxin binding, indicating a lack of α3 nicotinic receptor subunits in the SpL (Sorenson and Chiappinelli, 1992). Heterogeneity in these high-affinity nicotine receptors exists, as indicated by multiple conductances observed in cell-attached single channels recorded from SpL neurons (Weaver and Chiappinelli, 1996) and by whole-cell recording that revealed differences in sensitivities to the nicotinic antagonist trimethaphan (Weaver et al., 1994). On the other hand, all of the receptors exhibit very similar sensitivities to DHβE (Weaver et al., 1994). The cholinergic synapses mediating the evoked responses are likely to be on the dendrites of the SpL neurons, because the cholinergic fibers are associated predominantly with mAb35-immunopositive fibers.

In conclusion, we report that non-α7-containing nicotinic receptors mediate fast EPSPs that can generate action potentials in SpL neurons. The nicotinic cholinergic synapses appear to be on the dendrites of the SpL neurons rather than on the neuronal somas. Therefore, the SpL can be used as a model system in which to study the role of fast nicotinic neurotransmission in regulating the activity of neurons in the CNS.

REFERENCES

Alkondon M, Albuquerque EX (1993) Diversity of nicotinic acetylcholine receptors in rat hippocampal neurons. I. Pharmacological and functional evidence for distinct structural subtypes. J Pharmacol Exp Ther 265:1455–1473.

Alkondon M, Pereira EFR, Albuquerque EX (1998) α-Bungarotoxin- and methyllycaconitine-sensitive nicotinic receptors mediate fast synaptic transmission in interneurons of rat hippocampal slices. Brain Res 810:257–263.

Daubas P, Devillers-Thiery A, Geoffroy B, Martinez S, Bessis A, Changeux J-P (1990) Differential expression of the neuronal acetylcholine receptor alpha2 subunit gene during chick brain development. Neuron 5:49–60.

Frazier CJ, Buhler AV, Weiner JL, Dunwiddie TV (1998) Synaptic potentials mediated via α-bungarotoxin-sensitive nicotinic acetylcholine receptors in rat hippocampal interneurons. J Neurosci 18:8228–8235.

Johnson CD, Epstein ML (1986) Monoclonal antibodies and polyvalent antiserum to chicken choline acetyltransferase. J Neurochem 46:968–976.

McMahon LL, Yoon K-W, Chiappinelli VA (1994) Nicotinic receptor activation facilitates GABAergic neurotransmission in the avian lateral spiriform nucleus. Neuroscience 59:689–698.

Medina L, Reiner A, Veenman CL, Puelles L (1997) Identification of the anterior nucleus of the ansa lenticularis (ALa) in birds as the homologue of the mammalian subthalamic nucleus. Soc Neurosci Abstr 23:197.

Mizobe F, Livett BG (1982) Biphasic effect of eserine and other acetylcholinesterase inhibitors on the nicotinic response to acetylcholine in cultured adrenal chromaffin cells. J Neurochem 39:379–385.

Morris BJ, Hicks AA, Wisden W, Darlison MG, Hunt SP, Barnard EA (1990) Distinct regional expression of nicotinic acetylcholine receptor genes in chick brain. Mol Brain Res 7:305–315.

Reiner A, Brecha NC, Karten HJ (1982) Basal ganglia pathways to the tectum: the afferent and efferent connections of the lateral spiriform nucleus of pigeon. J Comp Neurol 208:16–36.

Roerig B, Nelson DA, Katz LC (1997) Fast synaptic signaling by nicotinic acetylcholine and serotonin 5-HT_3 receptors in developing visual cortex. J Neurosci 17:8353–8362.

Role LW, Berg DK (1996) Nicotinic receptors in the development and modulation of CNS synapses. Neuron 16:1077–1085.

Shaw K-P, Aracava Y, Akaike A, Daly JW, Rickett DL, Albuquerque, EX (1985) The reversible cholinesterase inhibitor physostigmine has channel-blocking and agonist effects on the acetylcholine receptor-ion channel complex. Mol Pharmacol 28:527–538.

Sorenson EM, Chiappinelli VA (1990) Intracellular recording in avian brain of a nicotinic response that is insensitive to κ-bungarotoxin. Neuron 5:307–315.

Sorenson EM, Chiappinelli VA (1992) Localization of ^{3}H-nicotine, ^{125}I-κ-bungarotoxin, and ^{125}I-α-bungarotoxin binding to nicotinic sites in the chicken forebrain and midbrain. J Comp Neurol 323:1–12.

Sorenson EM, Parkinson D, Dahl JL, Chiappinelli VA (1989) Immunohistochemical localization of choline acetyltransferase in the chicken mesencephalon. J Comp Neurol 281:641–657.

Swanson LW, Lindstrom J, Tzartos S, Schmued LC, O'Leary DDM, Cowan WM (1983) Immunohistochemical localization of monoclonal antibodies to the nicotinic acetylcholine receptor in chick midbrain. Proc Natl Acad Sci USA 80:4532–4536.

Tzartos SJ, Rand DE, Einarson BL, Lindstrom JM (1981) Mapping of surface structures of electrophorus acetylcholine receptor using monoclonal antibodies. J Biol Chem 256:8635–8645.

Ullian EM, Sargent PB (1995) Pronounced cellular diversity and extrasynaptic location of nicotinic acetylcholine receptor subunit immunoreactivities in the chicken pretectum. J Neurosci 15:7012–7023.

Veenman CL, Reiner, A (1994) The distribution of GABA-containing perikarya, fibers, and terminals in the forebrain and midbrain of pigeons, with particular reference to the basal ganglia and its projection targets. J Comp Neurol 339:209–250.

Watson JT, Adkins-Regan E, Whiting P, Lindstrom J, Podleski TR (1988) Autoradiographic localization of nicotinic acetylcholine receptors in the brain of the zebra finch (*Poephila guttata*). J Comp Neurol 274:255–264.

Weaver WR, Chiappinelli VA (1996) Single-channel recording in brain slices reveals heterogeneity of nicotinic receptors on individual neurons within the chick lateral spiriform nucleus. Brain Res 725:95–105.

Weaver WR, Wolf KM, Chiappinelli VA (1994) Functional heterogeneity of nicotinic receptors in the avian lateral spiriform nucleus detected with trimethaphan. J Pharmacol Exp Ther 46:993–1001.

Yum L, Wolf KM, Chiappinelli VA (1996) Nicotinic acetylcholine receptors in separate brain regions exhibit different affinities for methyllycaconitine. Neuroscience 72:545–555.